Journal Pre-proofs

Synergetics: the cooperative phenomenon in multi-compressions S-CO$_2$ power cycles

Enhui Sun, Jinliang Xu, Mingjia Li, Hangning Li, Chao Liu, Jian Xie

Please cite this article as: E. Sun, J. Xu, M. Li, H. Li, C. Liu, J. Xie, Synergetics: the cooperative phenomenon in multi-compressions S-CO$_2$ power cycles, *Energy Conversion and Management: X* (2020), doi: https://doi.org/10.1016/j.ecmx.2020.100042

Synergetics: the cooperative phenomenon in multi-compressions S-CO$_2$ power cycles

Enhui Sun[a], Jinliang Xu[a, b], Mingjia Li[c], Hangning Li[a], Chao Liu[a], Jian Xie[a, b]

a)   Beijing Key Laboratory of Multiphase Flow and Heat Transfer for Low Grade Energy Utilization, North China Electric Power University, Beijing 102206, China

b)   Key Laboratory of Power Station Energy Transfer Conversion and System, North China Electric Power University, Ministry of Education, Beijing, 102206, China

c)   Key Laboratory of Thermo-Fluid Science and Engineering of Ministry of Education, School of Energy & Power Engineering, Xi'an Jiaotong University, Xi'an, Shaanxi 710049, China

Abstract

Mature power plant uses regenerative steam Rankine cycle to achieve excellent performance, but there is a lack of general approach for gas Brayton cycle. Here, synergetics is introduced to construct multi-compressions S-CO$_2$ cycle for the first time. Our work starts from the analysis of recompression cycle (RC). RC is decoupled into two simple Brayton cycles (SCs). We show that at the optimal split ratio of flow rate, the mixing stream coming from the two subsystems does not generate exergy destruction, and the heat transfer induced exergy destruction is controlled to an acceptable level. Thus, the two subsystems are synergistic to have the efficiency reinforcing feedback. This finding inspires us to construct multi-compressions cycle. For example, the tri-compressions cycle (TC) is built by cooperation between RC and SC, and the four-compressions cycle (FC) is formed based on TC and SC. At the main vapor parameters 550 ℃/20 MPa, thermal efficiencies are increased from 47.43% for RC to 49.47% for TC. A regime map is presented to select multi-compressions cycle based on main vapor parameters. We state that both of multi-compressions and reheating are effective. The combination of both approaches further improves system performance, but multi-compressions are preferable because the high temperature induced heat transfer issue can be avoided. This work fills the gap on how to reach excellent performance for gas Brayton cycle driven by various heat sources such as nuclear energy, solar energy and fossil energy etc.

Keywords: supercritical carbon dioxide (S-CO$_2$) cycle; synergetics; thermal efficiency; multi-compressions; renewable energy.

1. Introduction

Supercritical carbon dioxide cycle (S-CO$_2$ cycle) can be driven by nuclear energy, solar energy, fossil energies (coal/nature gas) [1–3]. Due to higher efficiency and compact system, S-CO$_2$ cycle may partially replace the widely used water-steam Rankine cycle in the future. Currently, the main vapor parameters entering the main turbine are set as 550 ℃/20 MPa, 700 ℃/25 MPa and 620 ℃/30 MPa for S-CO$_2$ cycles driven by nuclear energy [4,5], solar energy [6,7] and coal combustion [8,9], respectively. Specified by the temperature endurance limit of materials, the main vapor parameters cannot be randomly increased to improve the cycle efficiency. Thus, the cycle diversity and optimization have been pursued to raise the cycle efficiency.

Feher [10] proposed the simple recuperated cycle (SC) in 1968. Angelino [11,12] presented the pre-compression cycle (PC), recompression cycle (RC), split expansion cycle (SEC) and partial cooling cycle (PCC). In 1980s, the S-CO$_2$ cycles for nuclear energy and shipboard applications were investigated [13,14], and the effectiveness of the cycle through experiments was attempted to be verified [15,16]. In this period, the cycle optimization was emphasized without inventing new S-CO$_2$ cycles. Since 2000, S-CO$_2$ cycles attract many interests from both academic community and industry. Massachusetts Institute of Technology (MIT) [4], Argonne National Laboratory [17], Sandia National Laboratory [18], Tokyo Institute of Technology [19], Xi'an Jiaotong University (China) [3] and North China Electric Power university (China) [9] are the examples to investigate S-CO$_2$ cycles. In these studies, RC and SC are the basic cycles. Wang et al. [20] studied solar energy driven S-CO$_2$ cycle, showing that RC with intercooling can decrease the power consumption of compressor to increase the cycle efficiency. Osorio [21] showed that for solar energy application, SC with intercooling and reheating can have 0.7% efficiency improvement compared to SC without intercooling and reheating.

For S-CO$_2$ coal fired power plant, the coupling issue between cycle and heat source becomes serious. Usually, S-CO$_2$ cycle is suitable to extract heat from moderate or high temperature heat source, but flue gas covers a very wide temperature range of 1500−120 ℃ [22]. Using a single S-CO$_2$ cycle alone is difficult to extract flue gas heat for wide temperature range applications. Thus, the classical RC cycle is modified to overcome this issue. Moullec [8] used RC to extract high temperature (above 500℃) flue gas heat, but extracted part of the CO$_2$ flow rate from the

lowest temperature point of the cycle to absorb low temperature flue gas heat. After being heated, the branch CO_2 stream returns to the main RC cycle. Sun et al. [23] proposed a hybrid cycle to cascade utilize flue gas energy. Flue gas energies in high and low temperature ranges are absorbed by a top $S-CO_2$ cycle and a bottom $S-CO_2$ cycle, respectively. A new cycle, called SHC, was proposed to have better performance when it is used in low temperature range. The objective of these works is to develop methods for cascade utilization of flue gas heat, which is necessary for fossil energy applications due to wide temperature range, but not needed for solar or nuclear energy applications due to narrow temperature range.

To increase the thermal efficiency, the first law of thermodynamics tells us that when the total heat absorption is fixed, the heat dissipation to environment shall be decreased as small as possible. The second law of thermodynamics tells us that the exergy destructions of component and system shall be reduced as small as possible. Both of first and second laws of thermodynamics present the improvement direction of the cycle, but do not indicate how to design the cycle. After one century evolution, water-steam Rankine cycle has been widely used. How does a water-steam Rankine cycle attain high efficiency? The multi-stages regenerative heating is the secret to reach the power generation efficiency of 47%, in which steam enters the turbine to expand for power generation [24]. After vapor expansion to a specific degree, some steam is extracted from main vapor and routed to a regenerative heat exchanger to warm up feedwater (called feedwater heater), while the remaining steam continues to expand. The steam extraction/regenerative heating process is repeated by several times. Thus, the feedwater temperature entering boiler is raised to elevate the heat absorption temperature. The better performance of regenerative Rankine cycle can be understood based on the first law of thermodynamics. During regenerative heating, the extracted steam dissipates heat to feedwater, not to environment (final heat sink). In such a way, only part of the cycling flow rate dissipates heat to environment. Thus, the total heat dissipation to environment is decreased to save energy. The multi-stages regenerative cycle is a general principle to increase efficiency for steam Rankine cycle.

It is known that mature power plant uses multi-stages regenerative water-steam Rankine cycle to reach excellent performance. However, there does not exist a general approach for $S-CO_2$ cycle. To fill the knowledge gap, synergetics is introduced to construct multi-compressions $S-CO_2$

cycle for efficiency improvement. Our work starts from the analysis of recompression cycle (RC), which is decoupled into two simple Brayton cycles. We show that the cooperation between the two simple Brayton cycles decreases the heat dissipation to environment. Thus, the RC efficiency is better than the simple Brayton cycle. Besides, the cooperation of the two simple systems does not generate extra exergy destruction. The outcome inspires us to construct three or four compressions S-CO_2 cycles. Based on main vapor parameters, a regime map is presented to determine the optimal stages of multi-compressions cycle. The combined approach incorporating multi compressions and reheating is demonstrated to be effective, but multi-compressions are preferable because the high temperature induced heat transfer issue can be avoided when multi-compressions are used alone.

2. The scope and assumptions of the present paper

We aim to present a general principle to raise thermal efficiencies of S-CO_2 cycles, which is suitable for various heat sources such as nuclear energy, solar energy and fossil energy. Thus, we focus on the theoretical analysis, not focusing on the technical design of component and system, but the simplification does not influence the major conclusions drawn in this study. Because turbines and compressors have different isentropic efficiencies for different power capacities of the system, the system thermal efficiency is dependent on power capacities. The present paper focuses on larger scale power plant analysis with power capacities in the range of 100-1000 MWe, under which the axial type compressors and turbines are recommended and they have higher isentropic efficiencies [25]. In other words, large scale power plant is insensitive to the variation of the component performances. Thus, the system is scaled by the unit mass flow rate of CO_2 (1 kg/s). Besides, the present paper is performed for the steady operation of the system. Small scale power plant, off-design and transient operation of S-CO_2 cycle is beyond the scope of the present paper, but will be investigated in the future.

Regarding the power plant design, there are many technical issues should be tackled. However, the objective of this paper is to examine how and why the system efficiency is improved by consecutively adding a simple Brayton cycle to its mother cycle. Thus, S-CO_2 cycles with different compression stages should be compared with the same characteristic parameters for a specific type component. Using different isentropic efficiencies of turbines or compressors makes

the comparison meaningless. The major assumptions are summarized as follows:

The system efficiency: Thermal efficiency of the system η_{th} is defined as the useful mechanical power divided by the heat absorption from the heat source. The power efficiency η_e is related to other efficiency components as $\eta_e = \eta_{th}\eta_h\eta_p\eta_g$, where η_h, η_p and η_g are the heat source efficiency (heater), pipeline efficiency and generator efficiency. η_h depends on which type of heat source used. For coal fired power plant, η_h can be 93.5% [26]. For large scale power plant, the pipeline efficiency and generator efficiency can be 99% and 98.5%, respectively [9,27,28]. Because these efficiencies except thermal efficiency are the same for different cycle designs, the comparison regarding the thermal efficiency is sufficient when one deals with S-CO$_2$ cycles incorporating different compression stages in this paper. In power plant, the power consumption of lubricating oil systems, rotor cooling systems, cooling water systems, etc. is usually classified as the auxiliary services of thermal power plants [29,30]. This paper focuses on the thermodynamic analysis. Thus, the auxiliary services of thermal power plants are not considered.

Heat losses of each component: In a S-CO$_2$ cycle, components are divided into heater, regenerative heat exchanger such as HTR and LTR, compressor, turbine and cooler. Larger scale heater has higher heat absorption efficiency such as η_h=93.5% for coal combustion [26], but may be slightly changed for nuclear or solar energy applications. Because we focus on the system thermal efficiency, neglecting the η_h variation does not influence the major conclusion drawn in this paper. HTR and LTR use printed circuit heat exchangers, which are sufficient compact to have very small surface area exposed in the air environment relative to power capacity of the system. Thus, the heat losses of HTR and LTR are not considered in thermodynamics analysis [31–33]. Compressor or turbine do have the heat loss to the environment. However, there are no reliable data to predict the heat loss of these machines dependent on power capacities. In thermodynamics analysis for turbomachines, the heat loss is comprehensively reflected by the isentropic efficiency of the machine [6,8,34]. Cooler dissipates extra heat to the environment, which is definitely considered in this paper. In the cooler, the CO$_2$ fluid is cooled to a sufficiently lower temperature of 32 ^{o}C by the external environment fluid such as air or cooling water, which is 12 ^{o}C higher than a referenced environment temperature of 20 ^{o}C. The off-design condition will change the heat dissipation to the environment, but is beyond the scope of the present paper.

Characteristic parameters of various components: We focus on the analysis of large scale power plant with the power capacities in the range of 100-1000 MWe. The component performance is assumed to be independent on power capacities. Thus, the comparison among different system designs is possible and valuable. There are several characteristic parameters for the analysis. Because large scale axial type compressors and turbines are recommended, all the turbines and compressors have the isentropic efficiencies of 0.93 and 0.89, respectively, which are cited from Refs. [6,8,34]. These values are used throughout the present paper. Besides, pinch temperatures are the characteristic parameters for HTR and LTR, which are assumed to be 10 K in the present paper. The *T-Q* curves of HTR and LTR will be presented in latter section. Table 1 summarized the most important parameters for the components involved in the present study. Physical properties of CO_2 come from the NIST software REFPROP, which is widely used for cycle analysis [35].

3. The analysis of RC based on synergetics

3.1 Decoupling of RC and calculation procedure

Synergetics is a field of interdisciplinary research which is successful in revealing common features of diverging disciplines. There are many analogies between different phenomena in physics, astrophysics, chemistry, biology, sociology, economics [36–42]. These analogies become apparent when we adopt a certain level of abstraction and if we focus our attention on the most interesting phenomena, namely when dramatic qualitative changes of structures occur. In synergetics, an object is usually decomposed into subsystems, such as into atoms, molecules, cells, plants, human beings etc. One may observe that the subsystems cooperate in a well regulated way. The cooperation leads to macroscopic spatial or temporal structures or well defined processes. Furthermore, when specific external parameters are changed, the macroscopic structure or function may change dramatically. This change is called phase transition, which can be grouped into discontinuous or continuous transitions. A discontinuous transition (first order) is related to latent heat, hysteresis etc. A continuous transition (second order) is connected with a symmetry breaking instability, a soft mode, critical fluctuations etc. It turned out that completely analogous features are shared by quite other types of systems. Synergetics is applied in the present paper to explain why RC is better than the simple Brayton cycle. It guides us to construct multi

6

compressions S-CO_2 cycle for efficiency improvement.

Figure 1 shows the synergistic process, which helps us to invent new S-CO_2 cycles. Initially, both process A1 and A2 work independently, whose performances are represented by their own heights in Fig.1b. The synergy between A1 and A2 creates performance increment. After the 1st synergy, the performance B1 is greater than those of A1 and A2. Similarly, after the 2nd synergy, the performance C1 is larger than those of B1 and B2. In such a way, the synergy process can be continued to achieve more performance increments, which is similar to the reinforced extinction of species in nature [38].

Why RC is better than SC is explained based on synergetics. RC consists of a turbine T1 to generate mechanical work, a high temperature regenerative heat exchanger HTR, a low temperature regenerative heat exchanger LTR, a cooler for heat dissipation to environment, two compressors C1 and C2 for CO_2 compression, and a heater for heat absorption from heat source (see Fig.2a). HTR and LTR are for internal heat recycling. The total flow rate is separated into two streams at point 8. One stream flows through the cooler and is then compressed by C1. The remaining stream is compressed by C2 and then joins with the main stream at point 3. For convenient analysis, the cycle is scaled by a unit mass flow rate for total (m=1 kg/s), at which the flow rates entering C1 and C2 are $1-x_{C2}$ and x_{C2}, respectively, where x_{C2} is called the split ratio of flow rate.

Our analysis starts from the decoupling of RC into two coupled SC (see Fig.2b). In each SC, only one compressor is used. SC1 and SC2 work at the flow rate of $1-x_{C2}$ and x_{C2}, respectively. T1 is decoupled into T1(a) and T1(b): T1=T1(a)+T1(b). Similarly, heater, HTR and LTR shown in Fig.2a are decoupled into two parts of a and b shown in Fig.2b. Fig.2c shows the construction process. Fig.3 shows the T-Q/Q_{LTR} curves in LTR and T-Q/Q_{HTR} in HTR which clearly shows the heat transfer process in LTR and HTR of the recompression cycle.

The performances of RC, SC1 and SC2 should be determined (see Fig.4 for the procedure). Except $\eta_{C,s}$, $\eta_{T,s}$, ΔT_{LTR} and ΔT_{HTR}, the parameters at turbine inlet (T_5/P_5) and compress C1 inlet (T_1/P_1) are known. The initial step is to determine x_{C2} based on RC. The definition of the isentropic efficiency for T1 yields

$$\eta_{T1,s} = \frac{h_5 - h_6}{h_5 - h_{6,s}} \tag{1}$$

where $h_{6,s}$ is the enthalpy based on isentropic expansion, which is calculated by $s_{6,s}$ and P_6 using the REFPROP software. When a turbine undergoes an isentropic process, $s_{6,s}$ is equal to the turbine inlet entropy s_5. The enthalpy at turbine outlet, h_6, can be determined by Eq.1, noting that the numerator of right-hand-side of Eq.1 is the work output by T1. Similarly, the enthalpy at C1 outlet, h_2, can be decided based on the isentropic efficiency of C1:

$$\eta_{C1,s} = \frac{h_{2,s} - h_1}{h_2 - h_1} \tag{2}$$

Where $h_{2,s}$ is the enthalpy based on the isentropic compression, which is calculated by $s_{2,s}$ and P_2 using the software REFPROP. When a compressor undergoes an isentropic process, $s_{2,s}$ is equal to the compressor inlet entropy s_1. The power consumption by C1 is

$$w_{C1} = (1 - x_{C2})(h_2 - h_1) \tag{3}$$

The enthalpy at C2 outlet, h_3, can be calculated based on the following equation:

$$\eta_{C2,s} = \frac{h_{3,s} - h_8}{h_3 - h_8} \tag{4}$$

The power consumption by C2 is

$$w_{C2} = x_{C2}(h_3 - h_8) \tag{5}$$

The energy conservation equation across the two sides of HTR writes

$$h_6 - h_7 = h_4 - h_3 \tag{6}$$

The pinch temperature criterion for LTR satisfies that

$$\begin{cases} T_8 = T_2 + \Delta T_{LTR} \\ T_7 = T_3 + \Delta T_{LTR} \end{cases} \tag{7}$$

The energy conservation equation across the two sides of LTR writes

$$h_7 - h_8 = (1 - x_{C2})(h_3 - h_2) \tag{8}$$

Equation 8 results in x_{C2} as

$$x_{C2} = 1 - \frac{h_7 - h_8}{h_3 - h_2} \tag{9}$$

After x_{C2} is determined, the performance of RC is defined as

$$
\begin{cases}
q_h = h_5 - h_4 \\
w_{T1} = h_5 - h_6 \\
q_c = (1 - x_{C2})(h_8 - h_1) \\
\eta_{th,RC} = \dfrac{w_{T1} - w_{C1} - w_{C2}}{q_h}
\end{cases}
\tag{10}
$$

Where q_h is the heat absorption by RC, scaled by 1 kg/s mass flow rate of CO_2. q_c is the heat dissipated by cooler. The performances of SC1 and SC2 are

$$
\begin{cases}
q_{h,\,SC1} = (1 - x_{C2})(h_5 - h_{4'}) \\
w_{T1,\,SC1} = (1 - x_{C2})(h_5 - h_6) \\
w_{C1,\,SC1} = (1 - x_{C2})(h_2 - h_1) \\
\eta_{th,\,SC1} = \dfrac{w_{T1,\,SC1} - w_{C1,\,SC1}}{q_{h,\,SC1}}
\end{cases}
\tag{11}
$$

$$
\begin{cases}
q_{h,\,SC2} = x_{C2}(h_5 - h_4) \\
w_{T1,\,SC2} = x_{C2}(h_5 - h_6) \\
w_{C2,\,SC2} = x_{C2}(h_3 - h_8) \\
\eta_{th,\,SC2} = \dfrac{w_{T1,\,SC2} - w_{C2,\,SC2}}{q_{h,\,SC2}}
\end{cases}
\tag{12}
$$

Equations 11-12 imply that the total heat absorption q_h is assigned to the two subsystems as $q_{h,\,SC1}$ and $q_{h,\,SC2}$. The total work output w_{T1} is also decoupled into $w_{T1,\,SC1}$ and $w_{T1,\,SC2}$.

3.2 Why is RC better than SC

Figure 5a–c shows the T–s curves for RC, SC1 and SC2 with T_5=620 ℃ and P_5=30 MPa, identifying the performance difference among the three cycles, where s is the fluid entropy. We show that at $x_{C2} = 0.335$, the thermal efficiency is 51.55% for RC, which is larger than 44.86% for SC1 and 36.21% for SC2. From synergetics point of view, the cooperation between SC1 and SC2 generates performance amplification. The phase transition occurs at the critical condition $x_{C2} = 0.335$.

In order to explain why RC is better than any of the two subsystems, x_{C2} is treated as a variable varying in the range of 0–0.7. Thus, RC, SC1 and SC2 should be recalculated. Figure 5d

9

focusses on the mixing point 3 for RC shown in Fig.2a. Two CO_2 streams enter point 3. One stream from C1 has the mass flow rate $1-x_{C2}$ and temperature T_{3a}. The other stream from C2 has the mass flow rate x_{C2} and temperature T_{3b}. The complete mixing of the two streams results in the temperature T_3:

$$h_3 = \left(1-x_{C2}\right)h_{3a} + x_{C2}h_{3b} \tag{13}$$

where h_{3a} and h_{3b} are the enthalpies based on T_{3a} and T_{3b}, respectively. T_3 can be determined based on h_3 and P_3. Figure 5d illustrates that T_{3a}, T_{3b} and T_3 are different when $x_{C2} < 0.335$, yielding significant exergy destruction due to mixing. The difference among the three temperatures decreases when x_{C2} approaches 0.335. Alternatively, the conditions $x_{C2} > 0.335$ are paid attention, under which the three temperatures are identical ($T_{3a}=T_{3b}=T_3$), and the mixing induced exergy destruction does not exist. However, the heat transfer induced exergy destruction becomes another issue. We note that the side point temperature difference is defined as $\Delta T = T_8 - T_2$ for LTR. ΔT abruptly increases when $x_{C2} > 0.335$ (see Fig.5e). Thus, the heat transfer induced exergy destruction greatly raises in LTR, under which the pinch temperature criterion cannot be satisfied anymore. Thus, we conclude that the best RC performance can only occur at the critical split ratio of flow rate, which has also been discussed by others [8,17,43]. Our results in the following are calculated under the critical split ratio.

The better RC performance than SC can be stated as follows. Independently, the thermal efficiencies are 44.86% for SC1 and 36.21% for SC2. However, if SC1 and SC2 are considered as a whole, the cooperation between the two subsystems ensures SC2 to have the efficiency of 1. This is because SC2 dissipates extra heat to SC1, not to environment. RC can be thought as a Brayton cycle SC1 cooperating with another Brayton cycle SC2. The internal heat recycling ensures RC to have an amplifying feedback. Then, the better RC performance can be obtained with the well cooperative of the two subsystems.

4. Multi-compressions S−CO_2 cycle

The analysis of RC inspires us to construct multi-compressions S-CO_2 cycle. The triple-compressions S-CO_2 cycle (TC) is constructed by adding a simple recuperated cycle SC3 to

10

a recompression cycle RC (see Fig.6). The total flow rate, scaled as 1 kg/s, flows through the heater and the turbine T1. Due to three compressors used, partial flow rate flows through each compressor: $1 - x_{C2} - x_{C3}$ in C1, x_{C2} in C2 and x_{C3} in C3. Correspondingly, three regenerative heat exchangers, HTR in high temperature range, MTR in moderate temperature range, and LTR in low temperature range are arranged. For synergistic analysis, the heater is decoupled into heater (a) and heater (b). Similar decoupling process is performed for HTR and MTR, but LTR is not necessary to be decoupled.

Basically, TC includes two subsystems of RC and SC3 (see Figs.6-7). Because three SC cycles are involved in TC, the optimal condition yields the flow rates of 0.5687 in SC1, $x_{C2} = 0.2866$ in SC2, and $x_{C3} = 0.1447$ in SC3. The three processes of compressions are 1–2, 10–3 and 9–4. Correspondingly, the three regenerative heat transfer processes are as follows: 9-10 is recycled to 2-3, 8-9 is recycled to 3-4, and 7-8 is recycled to 4-5. We found that TC has the thermal efficiency of 52.54%, which is larger than 51.55% for RC. This indicates that the synergistic cooperation between RC and SC3 generates a net efficiency increment. We note that if one considers SC3 independently, SC3 has the low efficiency of 14.16%, but the efficiency amplifying still occurs due to the internal heat recycling. We emphasize that the above conclusion is valid at the optimal condition. In fact, TC was mentioned by Moisseytsev and Sienicki [17], who did not observe the efficiency benefit when using TC compared to RC. Their finding is explained here. The performance reinforcing effect is deteriorated when deviating from the optimal condition, due to the increased mixing or heat transfer induced exergy destructions.

Figure 8 shows the four-compressions S-CO$_2$ cycle (FC), which was never reported in the literature. Figure 9a shows the general construction of multi-compressions S-CO$_2$ cycle. TC is formed by adding SC to RC, and FC is formed by adding SC to TC. It is known that multi-stages regenerative steam Rankine cycle increases the efficiency and has been widely used. Here, the proposed multi-compressions S-CO$_2$ cycle fills the gap on how to raise thermal efficiency for gas Brayton cycle. At the main vapor parameters of 620 ℃/30 MPa, thermal efficiencies are 44.86%, 51.55% and 52.54% for SC, RC and TC, respectively, demonstrating obvious efficiency reinforcing by continuous adding SC (see Figure 9b).

A question may arise for multi-compressions. Can multi-compressions be continued infinitely

by adding more and more SCs? What is the maximum stages of compressions? The *T-s* curves shown in Fig.10a answer this question. If the outlet temperature of final stage compressor is smaller than the temperature entering the heater, a multi-compressions $S-CO_2$ cycle is success. For RC, the final stage compression temperature and inlet temperature of heater are T_3 and T_4, respectively. Thus, a success RC shall satisfy the criterion $T_3 < T_4$ (see Fig.10a). Alternatively, the two temperatures are named as T_4 and T_5 for TC. A success TC shall satisfy the criterion $T_4 < T_5$ (see Fig.10b). Otherwise, the constructed TC is failed (see Fig.10c).

The main vapor parameters strongly influence the maximum stages of compressions. A regime map is presented with main vapor pressure (P_{mv}) as horizontal coordinate and main vapor temperature (T_{mv}) as vertical coordinate (see Fig.10d). For high pressure/low temperature operation, the criterion for multi-compressions is strict, which is not easy to be satisfied. We note that high pressure is generated by over-compression. Thus, the outlet temperature of compressor is increased to easily approach the temperature entering the heater. More stages compressions are not preferable, explaining why the SC region with single stage compression is populated in the right-bottom corner of the regime map (see red color in Fig.10d). On the contrary, the low pressure/high temperature operation is preferable for more stages compressions. For example, the FC region (four stages compressions) is populated in the left-top corner of the regime map (see grey color in Fig.10d). This is because the elevated heater temperature makes flexible choice to use multi-stages compressions, each stage having a lower compression ratio.

Figure 10d gives the guideline to select multi-compressions $S-CO_2$ cycle for different heat sources. For coal fired power plant, the main vapor pressure can be as high as ~30 MPa, and the vapor temperature is above 580 ℃ [24]. It is recommended to use TC due to its higher efficiency than RC. For nuclear energy or solar energy, the main vapor pressure is in the range of 20-25 MPa [4–7]. It is preferable to use TC for nuclear energy applications. For solar energy, $S-CO_2$ cycle can be divided into indirect and direct cycles. The indirect cycle has lower CO_2 temperature to drive turbine. In direct cycle, CO_2 directly flows through the heater to generate higher temperature vapor for power generation, accompanying serious heat transfer problem due to high heat flux irradiation [44–46]. For tower solar power generation, the indirect $S-CO_2$ cycle has the vapor temperature ~550 ℃, at which TC is suggested. Instead, FC with four stages compressions is

12

recommended for direct CO_2 cycle due to the high temperature ~700 °C.

5. Multi-compressions versus reheating/double-reheating

For water-steam Rankine cycle, reheating (RH) increases thermal efficiency and has been widely applied [24,47]. RH also improves thermal performance of S-CO_2 cycle [9]. Figure 11a shows RC incorporating RH or DRH (double reheating). The system can work in RC, RC+RH, or RC+DRH by switching on/off corresponding valves among V1, V2, V3 and V4. For example, the system works in RC mode by switching off all the valves from V1 to V4. Alternatively, it works in RC+RH mode by switching on V2 and V3 but switching off V1 and V4. By using RH or DRH, the improved efficiency is caused by the elevated heat absorption temperature, in which SH means single-heating shown in Fig.11a.

Figure 11b shows the regime map for multi-compressions S-CO_2 cycle incorporating reheating. Compared to Fig.10d, the multi-compressions S-CO_2 cycle with reheating significantly shortens the SC region, and shifts the transition boundaries between different regions to right. In other words, multi-compressions are easier to be implemented when embedding reheating. The enlarged region for more stages compressions can be explained by two factors. First, when reheating is available, the temperature difference between outlet and inlet of the heater decreases, elevating the inlet temperature of heater. Second, one notes that heater 2 and turbine T2 are beyond T1 (see Fig.11a). Such configuration does not affect the CO_2 temperature distribution before T1. The CO_2 temperature at the final stage compressor outlet is independent on whether RH is used. The comprehensive effect enlarges the temperature difference between the inlet temperature of heater and the final stage compressor outlet temperature. In other words, if RH is incorporated in cycle, multis-compressions becomes easier to be implemented. Because multi-compressions S-CO_2 cycle with reheating further increases thermal efficiencies, Fig.11b is more useful than Fig.10d for practical applications.

The comprehensive effect of multi-compressions and reheating/double-reheating is further discussed in Fig.12. In order to do so, three groups of main vapor parameters are set as 550 °C/20 MPa, 700 °C/25 MPa and 620 °C/30 MPa. These parameters are practically useful for nuclear energy, solar energy and fossil energy (coal) applications. When RH/DRH is not involved, multi-compressions cycle increases thermal efficiencies, which is correct for any main vapor

parameters. The performance increment is more obvious from RC to TC than that from TC to FC. TC is strongly recommended for practical applications. Even though FC slightly increases thermal efficiency compared to TC, it needs an additional stage compression and regenerative heat transfer. Here, we recall the widely used water-steam Rankine cycle, which can have more stages of regenerative heat transfer (for example, 8-10 stages) [47,48]. For Brayton cycle, due to the temperature limit between the heater inlet temperature and the final stage compression temperature, adding a couple of more compression stages in the cycle are sufficient to improve the performance compared to RC.

Multi-compressions cycle incorporating RH further improves the performance. For example, at parameters of 550 °C/20 MPa, TC+RH cycle has the thermal efficiency 51.13%, which is larger than 49.47% for TC. Multi-compressions and reheating are two approaches for performance improvement. Multi-compressions set partial flows in different stages of compressors to minimize heat dissipation to environment, *belonging to the cold side approach*. Reheating elevates the heat absorption temperature, *belonging to the hot side approach.* Both approaches are effective. Figure 12 tells us that TC+RH is perfect to raise thermal efficiency. Modern power plant with steam Rankine cycle even considers double-reheating [24,48]. Recent study shows that the S-CO$_2$ Brayton cycle with double-reheating has efficiency benefit compared to the cycle with reheating [9]. However, double-reheating not only increases system complexity, but also generates pressure drop penalty in the heater, careful attention should be paid to use double-reheating.

A question arises between the selection of multi-compressions and reheating. Which one is preferable when only one approach is available? The answer is that we shall choose multi-compressions instead of reheating, which can be verified by Fig.12. For example, at the main vapor parameters 700 °C/ 25 MPa, TC has the efficiency 56.38%, exceeding the efficiency 56.08% for RC+RH. Besides, multi-compressions are easier to be implemented compared to reheating. Sometimes, reheating may cause heat transfer problem when the heater operates in high temperature region.

6. Conclusions

Following conclusions can be drawn:

1. Based on synergetics, RC is decoupled into two SCs. Our calculation shows that at optimal

split ratio of flow rare, the two subsystems are cooperative to have no mixing induced exergy destruction and acceptable heat transfer induced exergy destruction, yielding the improved performance of RC than a single SC.

2. The analysis of RC inspires us to construct multi-compressions S-CO$_2$ cycle. TC is built by cooperation between RC and SC, and FC is formed based on TC and SC. At the main vapor parameters 620 ^{o}C/30 MPa, TC has the efficiency 52.54%，which is larger than 51.55% for RC, showing apparent efficiency amplifying.

3. A success multi-compressions S-CO$_2$ cycle shall be limited by the criterion that the final stage compression temperature is lower than the inlet temperature of heater. For the system incorporating reheating, multi-compressions cycle is easier to be implemented.

4. Multi-compressions and reheating belong to the cold side approach and hot side approach, respectively. Both approaches are effective. TC+RH cycle is recommended for applications. Because multi-compressions cycle does not generate additional heat transfer problem, it is preferable compared to reheating.

5. Multi-compressions Brayton cycle can be analogized to regenerative steam Rankine cycle, filling the gap on how to explore the efficiency limit for gas Brayton cycle. The approach is suitable for various heat sources. The maximum stage of compressions can be determined by the regime map based on main vapor parameters.

Acknowledgements

Reference

[1]   Xu J, Liu C, Sun E, Xie J, Li M, Yang Y, et al. Perspective of S−CO$_2$ power cycles. Energy 2019;186:115831.

[2]   Crespi F, Gavagnin G, Sánchez D, Martínez GS. Supercritical carbon dioxide cycles for power generation: A review. Appl Energy 2017;195:152–83.

[3]   Li MJ, Zhu HH, Guo JQ, Wang K, Tao WQ. The development technology and applications of supercritical CO$_2$ power cycle in nuclear energy, solar energy and other energy industries. Appl Therm Eng 2017;126:255–75.

[4]   Dostal V, Driscoll MJ, Hejzlar P. A supercritical carbon dioxide cycle for next generation nuclear reactors. Ph.D. thesis. Massachusetts Institute of Technology, Department of Nuclear Engineering; 2004.

[5]   Li MJ, Xu JL, Cao F, Guo JQ, Tong ZX, Zhu HH. The investigation of thermo-economic performance and conceptual design for the miniaturized lead-cooled fast reactor composing supercritical CO_2 power cycle. Energy 2019;173:174–95.

[6]   Padilla RV, Too YCS, Benito R, Stein W. Exergetic analysis of supercritical CO_2 Brayton cycles integrated with solar central receivers. Appl Energy 2015;148:348–65.

[7]   Iverson BD, Conboy TM, Pasch JJ, Kruizenga AM. Supercritical CO_2 Brayton cycles for solar-thermal energy. Appl Energy 2013;111:957–70.

[8]   Le Moullec Y. Conceptual study of a high efficiency coal-fired power plant with CO_2 capture using a supercritical CO_2 Brayton cycle. Energy 2013;49:32–46.

[9]   Xu J, Sun E, Li M, Liu H, Zhu B. Key issues and solution strategies for supercritical carbon dioxide coal fired power plant. Energy 2018;157:227–46.

[10]   Feher EG. The supercritical thermodynamic power cycle. Energy Convers 1968;8:85–90.

[11]   Angelino G. Carbon dioxide condensation cycles for power production. J Eng Power 1968;90:287–95.

[12]   Angelino G. Real gas effects in carbon dioxide cycles. ASME 1969 gas turbine Conf. Prod. show, Citeseer; 1969, p. V001T01A071-V001T01A071.

[13]   Gokhshtein DP, Verkhivker GP. Use of carbon dioxide as a heat carrier and working substance in atomic power stations. At Energy 1969;26:430–2.

[14]   Combs O V. An investigation of the supercritical CO_2 cycle (Feher cycle) for shipboard application 1977.

[15]   Akagawa K, Fujii T, Sakaguchi T, Kawabata K, Ogura K, KURODA T, et al. Studies on Carbon Dioxide Power Plant: 1st Report, Experimental Results of Static Characteristics. Bull JSME 1980;23:238–46.

[16]   Hoffmann JR, Feher EG. 150 kwe supercritical closed cycle system. J Eng Power 1971;93:70–80.

[17]   Moisseytsev A, Sienicki JJ. Investigation of alternative layouts for the supercritical carbon

16

dioxide Brayton cycle for a sodium-cooled fast reactor. Nucl Eng Des 2009;239:1362–71.

[18] Pasch J, Carlson M, Fleming D, Rochau G. Evaluation of recent data from the Sandia National Laboratories closed Brayton cycle testing. ASME Turbo Expo 2016 Turbomach. Tech. Conf. Expo., American Society of Mechanical Engineers Digital Collection; 2016.

[19] Kato Y, Nitawaki T, Muto Y. Medium temperature carbon dioxide gas turbine reactor. Nucl Eng Des 2004;230:195–207.

[20] Wang K, He Y-L, Zhu H-H. Integration between supercritical CO_2 Brayton cycles and molten salt solar power towers: A review and a comprehensive comparison of different cycle layouts. Appl Energy 2017;195:819–36.

[21] Osorio JD, Hovsapian R, Ordonez JC. Dynamic analysis of concentrated solar supercritical CO_2-based power generation closed-loop cycle. Appl Therm Eng 2016;93:920–34.

[22] Sun E, Xu J, Hu H, Li M, Miao Z, Yang Y, et al. Overlap energy utilization reaches maximum efficiency for S-CO_2 coal fired power plant: A new principle. Energy Convers Manag 2019;195:99–113.

[23] Sun E, Xu J, Li M, Liu G, Zhu B. Connected-top-bottom-cycle to cascade utilize flue gas heat for supercritical carbon dioxide coal fired power plant. Energy Convers Manag 2018;172:138–54.

[24] Tumanovskii AG, Shvarts AL, Somova E V, Verbovetskii EK, Avrutskii GD, Ermakova S V, et al. Review of the coal-fired, over-supercritical and ultra-supercritical steam power plants. Therm Eng 2017;64:83–96.

[25] Sienicki JJ, Moisseytsev A, Fuller RL, Wright SA, Pickard PS. Scale dependencies of supercritical carbon dioxide Brayton cycle technologies and the optimal size for a next-step supercritical CO_2 cycle demonstration. Supercritical CO_2 power cycle symposium, 2011.

[26] Xu G, Xu C, Yang Y, Fang Y, Zhou L, Zhang K. Novel partial-subsidence tower-type boiler design in an ultra-supercritical power plant. Appl Energy 2014;134:363–73.

[27] Bai Z, Zhang G, Li Y, Xu G, Yang Y. A supercritical CO_2 Brayton cycle with a bleeding anabranch used in coal-fired power plants. Energy 2018;142:731–8.

[28] Hanak DP, Manovic V. Calcium looping with supercritical CO_2 cycle for decarbonisation of coal-fired power plant. Energy 2016;102:343–53.

17

[29] Ruiz AB, Cabello JM, Platero CA, Blázquez F. Multicriteria optimization of the investment in the auxiliary services of thermal power plants: A case study. Energy Convers Manag 2015;93:339–48.

[30] Mandi RP, Yaragatti UR. Control of CO_2 emission through enhancing energy efficiency of auxiliary power equipment in thermal power plant. Int J Electr Power Energy Syst 2014;62:744–52.

[31] Sarkar J. Second law analysis of supercritical CO_2 recompression Brayton cycle. Energy 2009;34:1172–8.

[32] Hou S, Wu Y, Zhou Y, Yu L. Performance analysis of the combined supercritical CO_2 recompression and regenerative cycle used in waste heat recovery of marine gas turbine. Energy Convers Manag 2017;151:73–85.

[33] Al-Sulaiman FA, Atif M. Performance comparison of different supercritical carbon dioxide Brayton cycles integrated with a solar power tower. Energy 2015;82:61–71.

[34] Halimi B, Suh KY. Computational analysis of supercritical CO_2 Brayton cycle power conversion system for fusion reactor. Energy Convers Manag 2012;63:38–43.

[35] Lemmon EW, Huber ML, McLinden MO. NIST Standard Reference Database 23, Reference Fluid Thermodynamic and Transport Properties (REFPROP), version 9.0, National Institute of Standards and Technology. R1234yf Fld File Dated December 2010; 22: 2010.

[36] Haken H. Synergetics. Phys Bull 1977;28:412.

[37] van der Sanden MCA, de Vries MJ. Science and Technology Education and Communication: Seeking Synergy. vol. 15. Springer; 2016.

[38] Brook BW, Sodhi NS, Bradshaw CJA. Synergies among extinction drivers under global change. Trends Ecol Evol 2008;23:453–60.

[39] Rhind JP. Aromatherapeutic blending: Essential oils in synergy. Singing Dragon; 2015.

[40] Yoshida M, Roh K, Mandal S, Bhaskar S, Lim D, Nandivada H, et al. Structurally controlled bio-hybrid materials based on unidirectional association of anisotropic microparticles with human endothelial cells. Adv Mater 2009;21:4920–5.

[41] Nabeshima T. Synergy in Supramolecular Chemistry. CRC Press, 2014.

[42] Farrugia LJ. The synergy between dynamics and reactivity at clusters and surfaces. vol. 465.

Springer Science & Business Media; 2012.

[43]   Sarkar J, Bhattacharyya S. Optimization of recompression S-CO$_2$ power cycle with reheating. Energy Convers Manag 2009;50:1939–45.

[44]   Zhu B, Xu J, Yan C, Xie J. The general supercritical heat transfer correlation for vertical up-flow tubes: K number correlation. Int J Heat Mass Transf 2020;148:119080.

[45]   Zhu B, Xu J, Wu X, Xie J, Li M. Supercritical "boiling" number, a new parameter to distinguish two regimes of carbon dioxide heat transfer in tubes. Int J Therm Sci 2019;136:254–66.

[46]   Fan YH, Tang GH, Li XL, Yang DL, Wang SQ. Correlation evaluation on circumferentially average heat transfer for supercritical carbon dioxide in non-uniform heating vertical tubes. Energy 2019;170:480–96.

[47]   Yang Y, Wang L, Dong C, Xu G, Morosuk T, Tsatsaronis G. Comprehensive exergy-based evaluation and parametric study of a coal-fired ultra-supercritical power plant. Appl Energy 2013;112:1087–99.

[48]   Li Y, Zhou L, Xu G, Fang Y, Zhao S, Yang Y. Thermodynamic analysis and optimization of a double reheat system in an ultra-supercritical power plant. Energy 2014;74:202–14.

Nomenclature			
C	compressor	TC	tri-compressions cycle
DRH	double reheating	T1(a)	part a of turbine 1
FC	four-compressions cycle	T1(b)	part b of turbine 1
h	specific enthalpy (kJ/kg)	V1-4	valve 1-4
HTR	high temperature regenerative heat exchanger	w	work done per unit mass flow rate (kJ/kg)
HTR(a)	part a of high temperature regenerative heat exchanger	x	split ratio of flow rate
HTR(b)	part b of high temperature regenerative heat exchanger		
LTR	low temperature regenerative heat exchanger	Subscripts	
LTR(a)	part a of low temperature regenerative heat exchanger	1, 2, 3...	state points of cycle
LTR(b)	part b of low temperature regenerative heat exchanger	C	compressor
m	mass flow rate (kg/s)	h	heater

MTR	moderate temperature regenerative heat exchanger	HTR	high temperature regenerative heat exchanger
MTR(a)	part a of moderate temperature regenerative heat exchanger	LTR	low temperature regenerative heat exchanger
MTR(b)	part b of moderate temperature regenerative heat exchanger	mv	main vapor
P	pressure	RC	recompression cycle
q	heat transfer per unit mass of a system (kJ/kg)	s	isentropic
RC	recompression cycle	SC	simple Brayton cycle
RH	reheating	T1	turbine 1
S-CO$_2$	supercritical carbon dioxide		
SC	simple Brayton cycle	Greek symbols	
SH	single-heating	$\eta_{C,s}$	isentropic efficiencies of compressor
syn	synergy	$\eta_{T,s}$	isentropic efficiencies of turbine
T	turbine	η_{th}	thermal efficiency
T	temperature	ΔT	pinch temperature

Table 1 S-CO$_2$ cycle parameters

Parameters	Values
turbine inlet temperature	550–700 °C
turbine inlet pressure	20–30 MPa
turbine isentropic efficiency (T1, T1(a), T1(b), T2 and T3)	0.93
compressor C1 inlet temperature (T_1)	32 °C
compressor C1 inlet pressure (P_1)	7.7 MPa
compressors isentropic efficiency (C1, C2, C3 and C4)	0.89
pinch temperature difference of LTR, MTR, MTR1, MTR2 and HTR	10 K

(a) Synergistic processes

Process: A   B   C --------- n
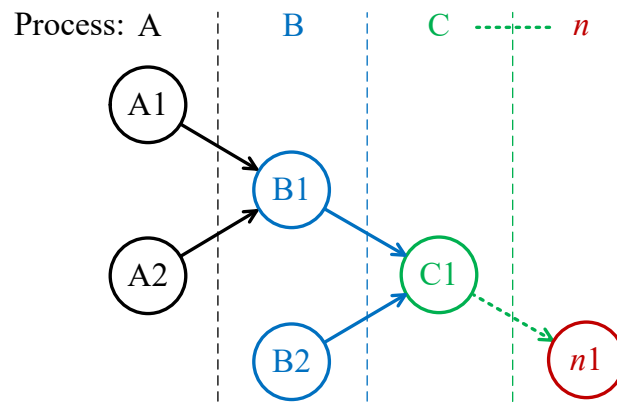
(b) Synergy changes the whole system performance
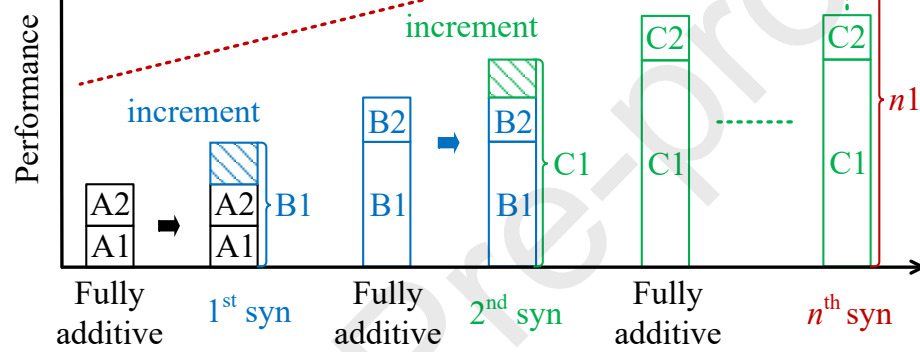
Figure 1 The steps for synergistic process with performance increment

(a) Recompression cycle (RC)

(b) Simple Bryton cycle 1 (SC1)

(c)

RC=SC1+SC2

Construction process:

T1(a)+T1(b)=T1

Heater (a)+Heater (b)=Heater

HTR (a)+HTR (b)=HTR

LTR (a)+LTR (b)=LTR

Simple Bryton cycle 2 (SC2)
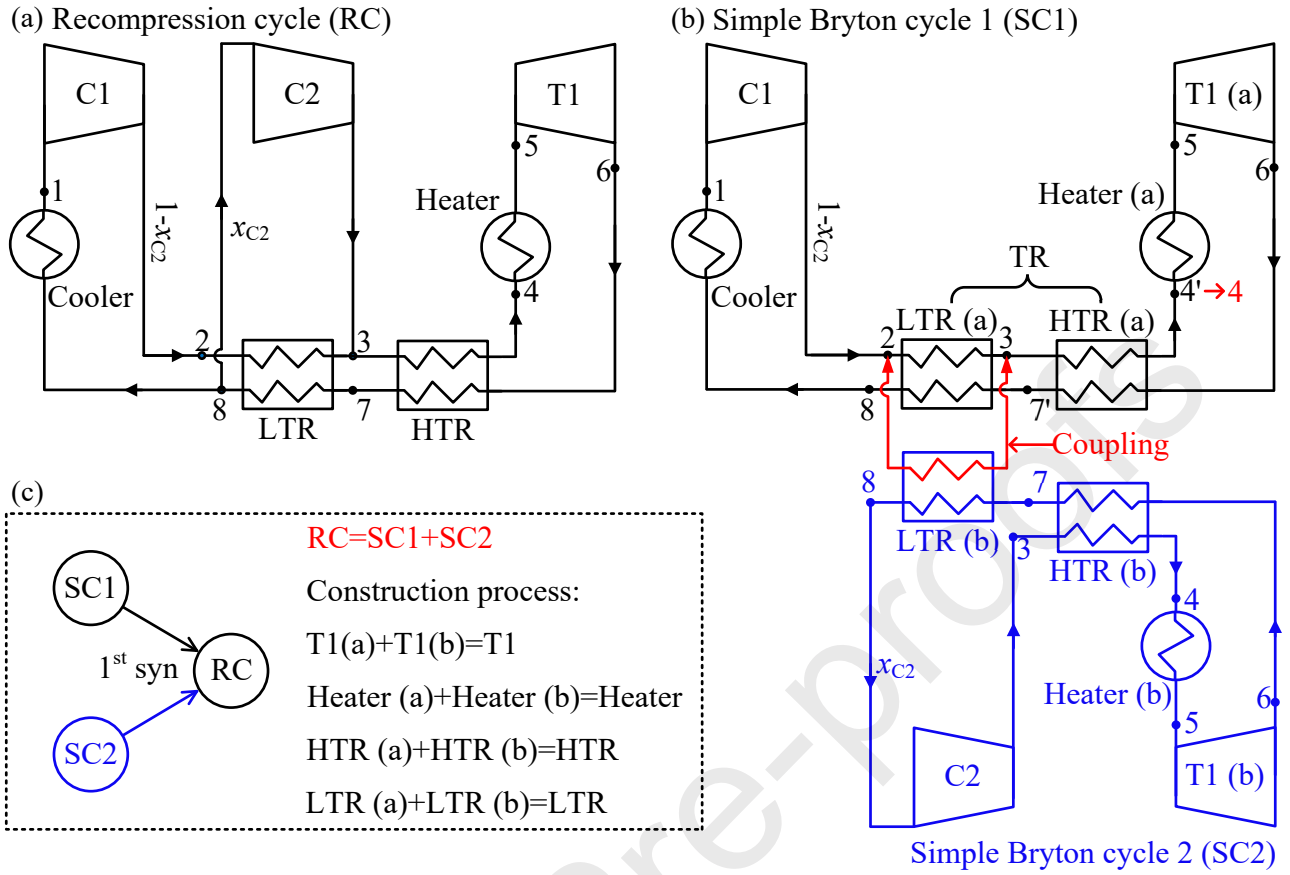
Figure 2 Decoupling of RC into two cooperative SC

23
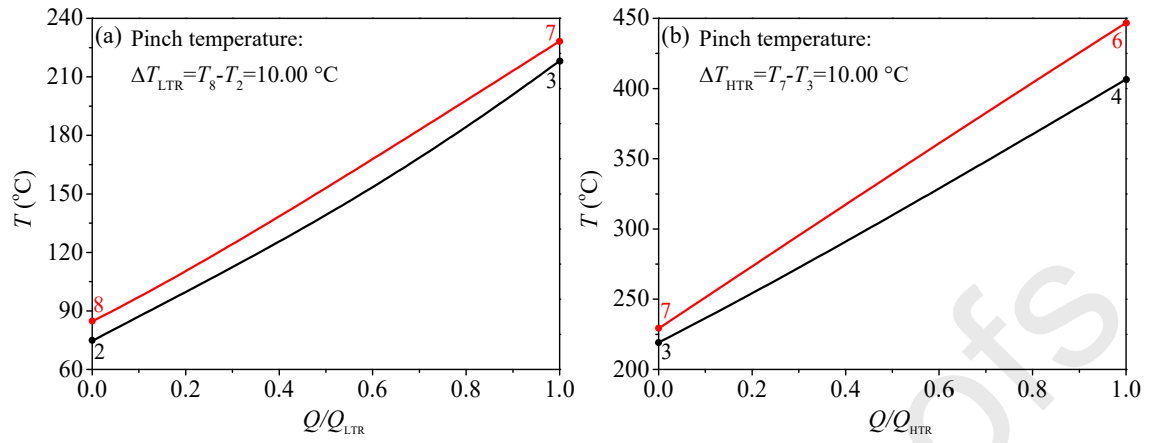
Figure 3 T-Q/Q_{TR} curves in LTR and HTR

```
                              ┌─────────┐
                              │  Start  │
                              └─────────┘
                                   │
              ╱──────────────────────────────────────╲
             ╱  Input: T₅, P₅, η_T,s, T₁, P₁,          ╲
            ╱   η_C,s, ΔT_LTR, ΔT_HTR                   ╱
           ╲──────────────────────────────────────────╱
                                   │
   ┌───────────────────────────────────────────────────┐
   │  Calculate h₆ by η_T1,s=(h₅-h₆)/(h₅- h₆,s)         │
   └───────────────────────────────────────────────────┘
                                   │
   ┌───────────────────────────────────────────────────┐
   │  Calculate h₂ by η_C1,s= (h₁- h₂,s)/(h₁-h₂)        │
   └───────────────────────────────────────────────────┘
                                   │
   ┌───────────────────────────────────────────────────┐
   │  T₈= T₂+ΔT_LTR                                      │
   └───────────────────────────────────────────────────┘
                                   │
   ┌───────────────────────────────────────────────────┐
   │  Calculate h₃ by η_C2,s= (h₈- h₃,s)/(h₈-h₃)        │   Based on RC
   └───────────────────────────────────────────────────┘
                                   │
   ┌───────────────────────────────────────────────────┐
   │  T₇= T₃+ΔT_LTR                                      │
   └───────────────────────────────────────────────────┘
                                   │
   ┌───────────────────────────────────────────────────┐
   │  Calculate h₄ by h₃-h₄=h₇-h₆                        │
   └───────────────────────────────────────────────────┘
                                   │
   ┌───────────────────────────────────────────────────┐
   │  x_C2=1-(h₇-h₈)/(h₃-h₂)                             │
   └───────────────────────────────────────────────────┘
```

Start

Input: T_5, P_5, $\eta_{T,s}$, T_1, P_1, $\eta_{C,s}$, ΔT_{LTR}, ΔT_{HTR}

Calculate h_6 by $\eta_{T1,s}=(h_5-h_6)/(h_5-h_{6,s})$

Calculate h_2 by $\eta_{C1,s}=(h_1-h_{2,s})/(h_1-h_2)$

$T_8=T_2+\Delta T_{LTR}$

Calculate h_3 by $\eta_{C2,s}=(h_8-h_{3,s})/(h_8-h_3)$

$T_7=T_3+\Delta T_{LTR}$

Calculate h_4 by $h_3-h_4=h_7-h_6$

$x_{C2}=1-(h_7-h_8)/(h_3-h_2)$

Based on RC

RC performance:
$q_h=h_5-h_4,$ $w_{T1}=h_5-h_6$
$w_{C1}=(1-x_{C2})(h_2-h_1)$
$w_{C2}=x_{C2}(h_3-h_8)$
$\eta_{th,RC}=(w_{T1}-w_{C1}-w_{C2})/q_h$

SC2 performance:
$q_{h,SC2}=x_{C2}(h_5-h_4)$
$w_{T1,SC2}=x_{C2}(h_5-h_6)$
$w_{C2,SC2}=x_{C2}(h_3-h_8)$
$\eta_{th,SC2}=(w_{T1,SC2}-w_{C2,SC2})/q_{h,SC2}$

Calculate $h_{4'}$ by $h_2-h_{4'}=h_8-h_6$

SC1 performance:
$q_{h,SC1}=(1-x_{C2})(h_5-h_{4'}),$
$w_{T1,SC1}=(1-x_{C2})(h_5-h_6)$
$w_{C1,SC1}=(1-x_{C2})(h_2-h_1)$
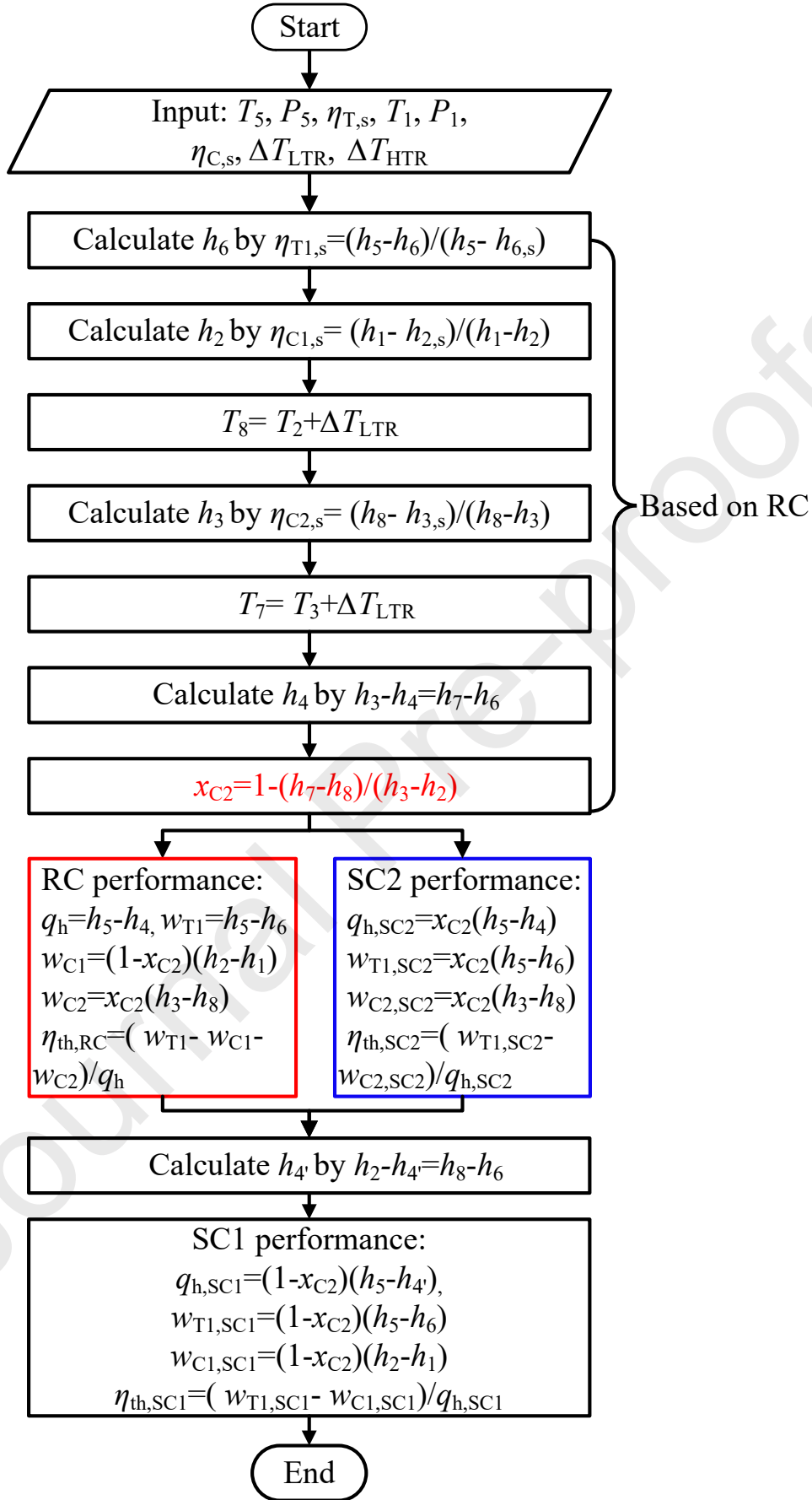$\eta_{th,SC1}=(w_{T1,SC1}-w_{C1,SC1})/q_{h,SC1}$

End

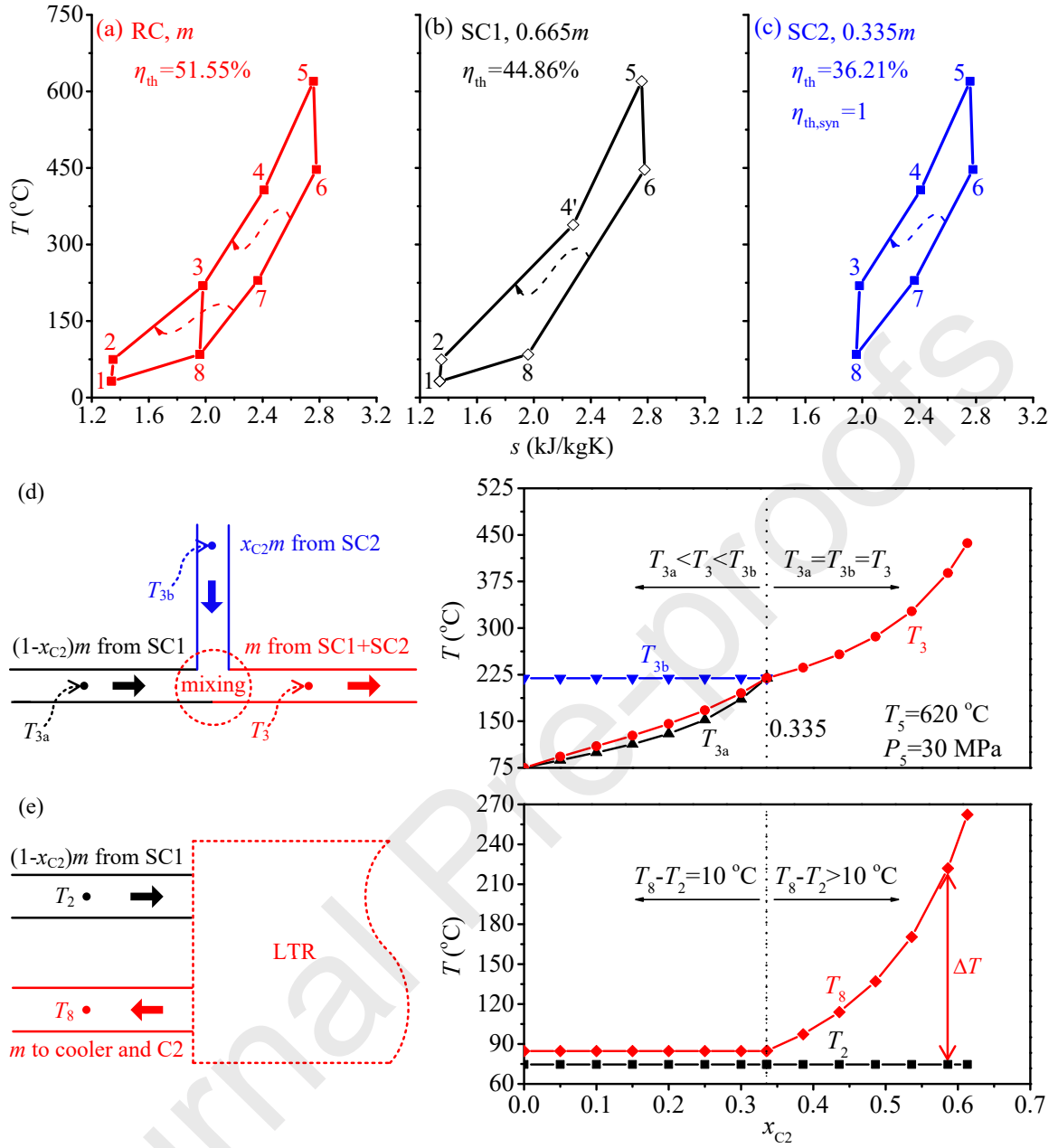Figure 4 The calculation procedure for RC and the decoupled subsystems

Figure 5 The cooperative SC1 and SC2 to form SC (a, b and c for $T–s$ curves of RC, SC1 and SC2 at optimal condition, d: the relationship between the three temperatures during mixing, e: the temperature difference at the side point of LTR)
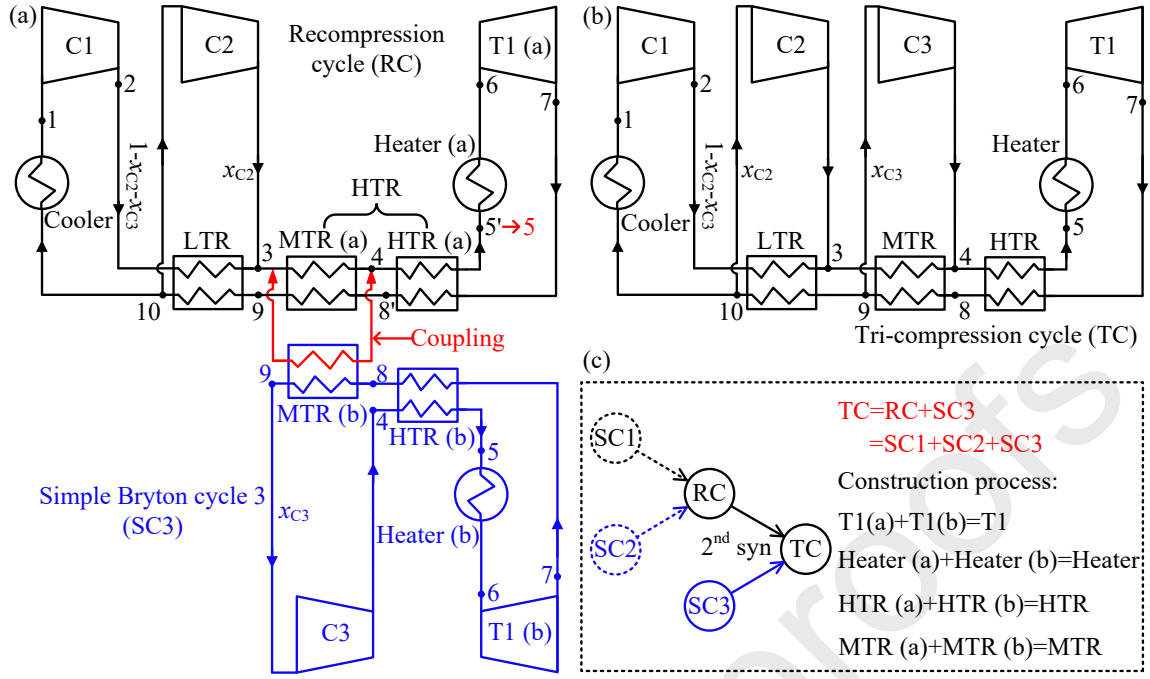
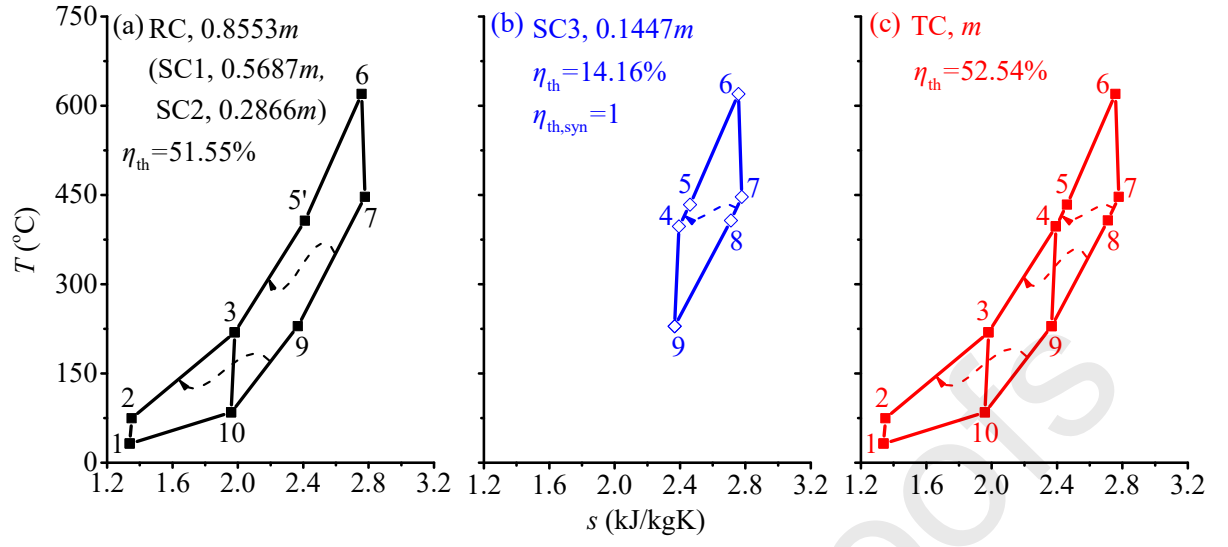Figure 6 The construction of TC based on synergetics

Figure 7 The relationship between TC and its two subsystems of RC and SC3
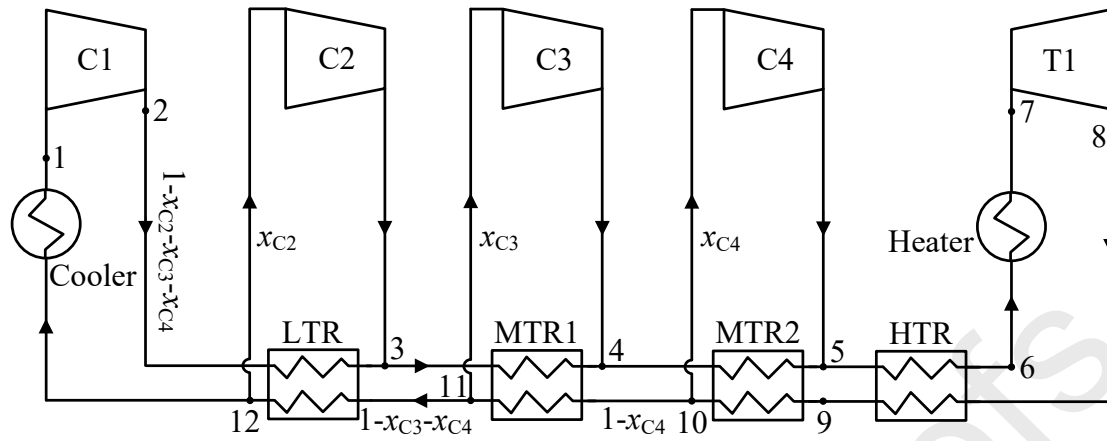
Four-compression cycle (FC)

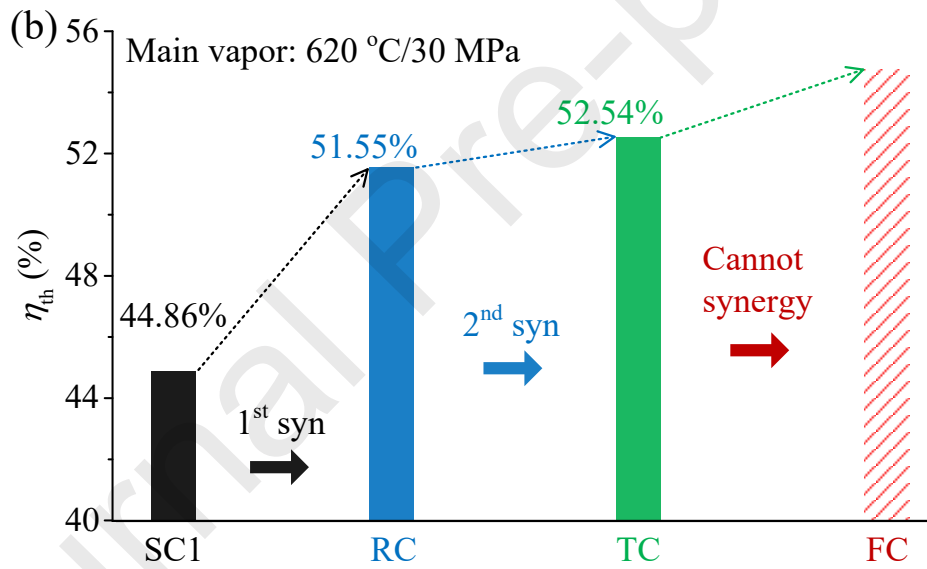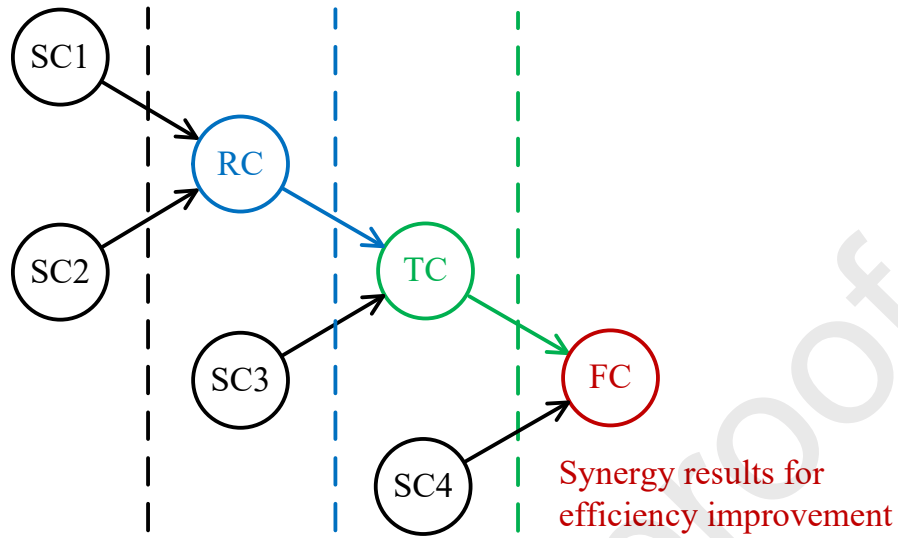Figure 8 The construction of FC based on synergetics

(a) Synergistic processes: SC to FC

(b)

Figure 9 The general principle to construct multi-compressions S-CO$_2$ cycle and the efficiency
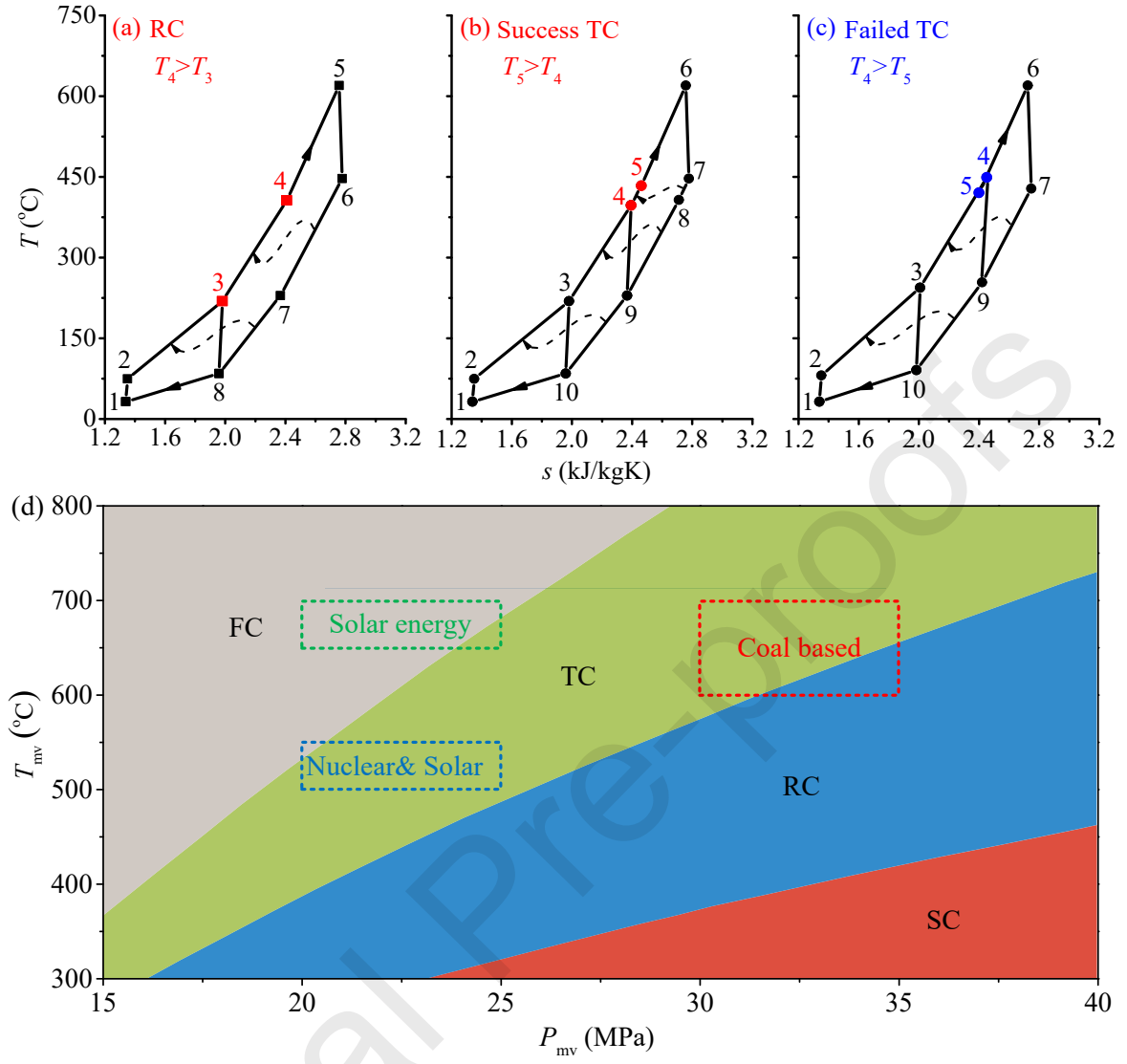
amplifying feedback

Figure 10 The criterion for success multi-compressions S-CO$_2$ cycle and the regime map
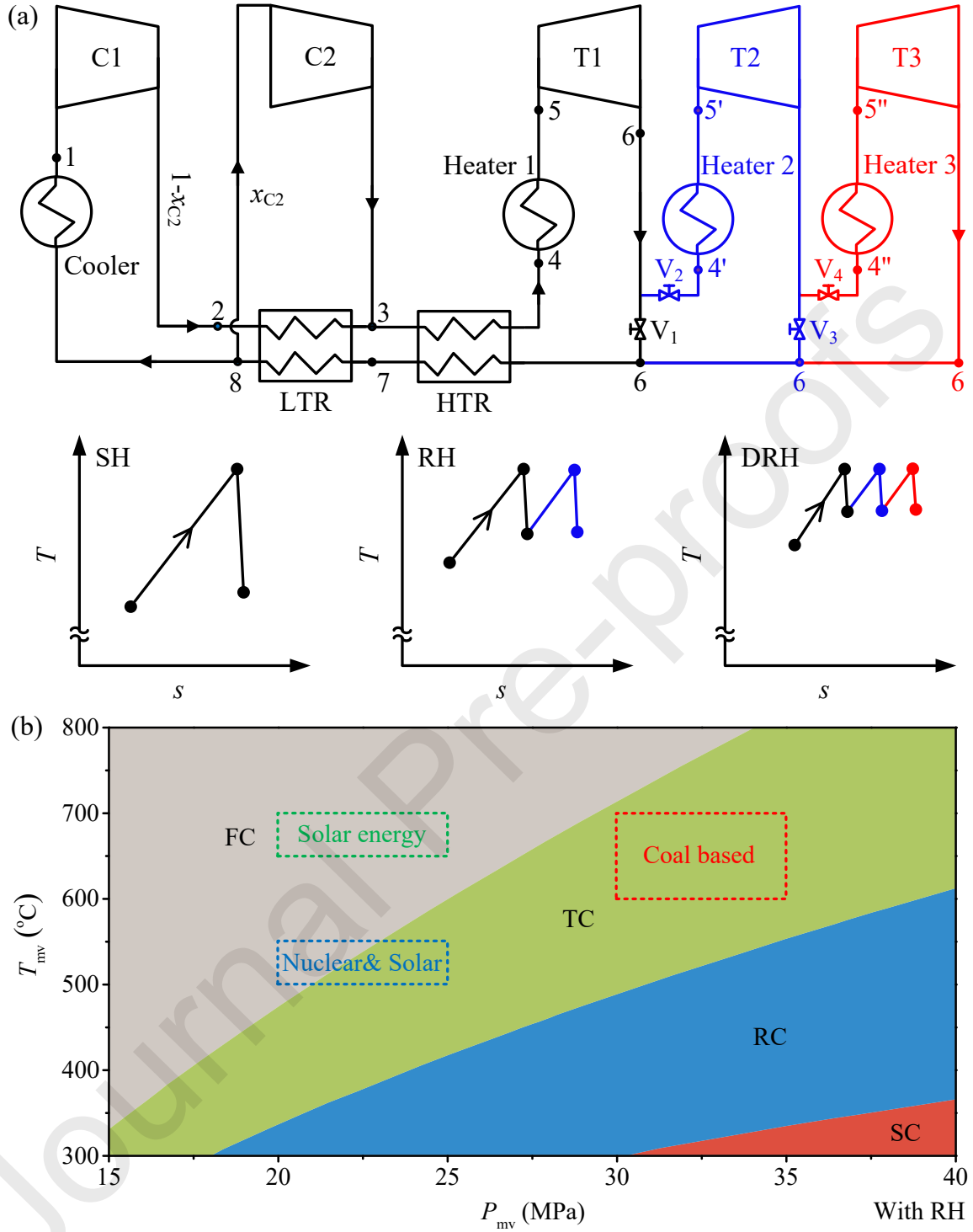
dependent on main vapor parameters

Figure 11 Multi-compressions S-CO$_2$ cycle with RH or DRH (a: RC with RH or DRH, b: regime

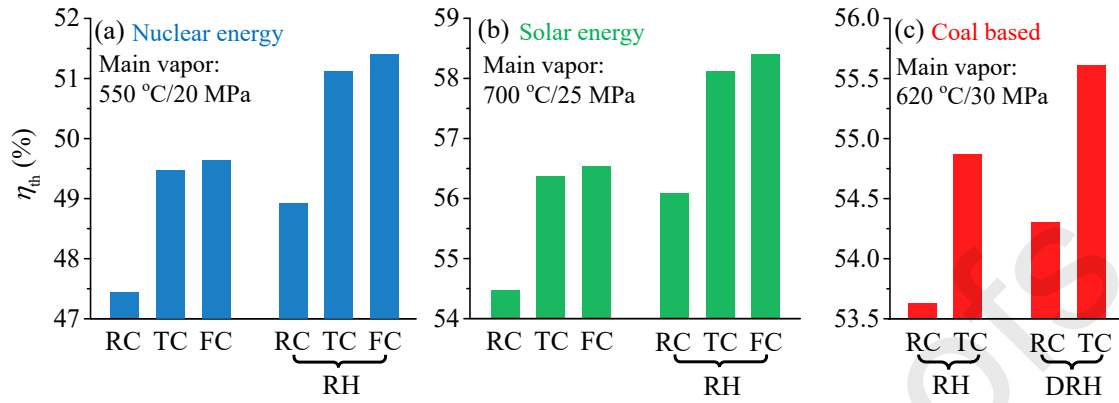map with S-CO$_2$ cycle incorporating RH)

Figure 12 The comprehensive effect by using multi-compressions and RH/DRH

Author statement

Dear Editor

We state that the paper titled as "Synergetics: the cooperative phenomenon in multi-compressions S-CO$_2$ power cycles" by Enhui Sun, Jinliang Xu, Mingjia Li, Hangning Li, Chao Liu, Jian Xie, submitted to Energy Conversion and Management, has not been published previously and will not be submitted to elsewhere before we receive your decision.

Best Regards

Jinliang Xu

North China Electric Power University, Beijing, China

Highlights

- Recompression cycle RC is decoupled into two simple Brayton cycles SCs.

- Cooperation in subsystems minimizes exergy destruction to yield efficiency amplifying.

- General strategy is proposed to construct multi-compressions S-CO$_2$ cycles.

- The maximum stage of compressions is limited by a well-defined temperature difference.

- One prefers multi-compressions instead of reheating when only one approach is available.